IRIS AperTO

UNIVERSITÀ DEGLI STUDI DI TORINO

AperTO - Archivio Istituzionale Open Access dell'Università di Torino

A new application of Curvatool semi-automatic approach to qualitatively detect geological lineaments

This is a pre print version of the following article:

Original Citation:

Availability:

This version is available http://hdl.handle.net/2318/1647552 since 2018-06-19T16:18:19Z

Published version:

DOI:10.2113/gseegeosci.23.3.179

Terms of use:

Open Access

Anyone can freely access the full text of works made available as "Open Access". Works made available under a Creative Commons license can be used according to the terms and conditions of said license. Use of all other works requires consent of the right holder (author or publisher) if not exempted from copyright protection by the applicable law.

(Article begins on next page)

12 October 2024

A new application of CurvaTool semi-automatic approach to qualitatively detect geological lineaments

***Bonetto Sabrina[a], Facello Anna[b], Umili Gessica[a]**

[a] Department of Earth Sciences, University of Turin, Valperga Caluso 35, 10125 Turin, Italy. {sabrina.bonetto, gessica.umili}@unito.it; 00390116705139

[b] CNR-IRPI, Strada delle Cacce,73 - 10135 Torino, Italy. anna.facello@irpi.cnr.it

*Corresponding author: Sabrina Bonetto, Department of Earth Sciences, University of Turin, Valperga Caluso 35, 10125 Turin, Italy. sabrina.bonetto@unito.it; 00390116705139

Abstract

In the ~~last few~~ past years, lineament analysis ~~is~~ has become an important analytical technique for delineation of major structural units in mineral prospecting, hydrogeology, and tectonic studies. The use of remote sensing, with progressive development of image enhancement techniques, provides an opportunity to produce more reliable and comprehensive lineament maps. In this paper, we propose the application of a semi-automatic approach based on Digital Terrain Models (DTM) for the extraction of potential lineaments and their detailed validation. We selected An area belonging to the Bagni di Vinadio municipality (Cuneo, NW Italy), which is part of the Argentera Massif (Western Alps), was selected as a test site. Data obtained from the code CurvaTool, developed by the authors, are successfully compared with literature information and with lineaments obtained from visual interpretation of remote sensing imagery. CurvaTool code permits the extraction and classification of a greater number of linear features ~~with respect~~ compared to visual interpretation techniques. The ability to detect features that are not perceptible by visual observation is a strong point ~~for~~ of CurvaTool processing. In the test area, CurvaTool output data correlate with visually detected linear features and show a good correlation with regional tectonics and iso-kinematic maps from the literature.

Keywords: Geological structure, Lineament extraction, DTM, Semi-Automatic survey, Argentera Massif

1 - INTRODUCTION

Detection and extraction of lineaments is an important step in analyses related to mineral prospecting, hydrogeology studies and tectonic studies to delineate major structural units, analyze structural deformation patterns, and identify geological boundaries (Clark and Wilson, 1994; Davis and Reynolds 1996; Rangzan et al., 2008; Lee et al., 2012). Usually, lineament maps created by field works cannot identify all the lineaments that exist in an area, due to the limited point of view of the mapper with respect to the geological structures. Field work can be a time consuming, expensive and sometimes a dangerous undertaking. Therefore, any technique that can make field work more efficient is thus beneficial.

In the past few years the use of remote sensing products, coupled with progressive development of image enhancement techniques, has provided scientists with a fast and relatively cheap way to gather information that complements classical field geology. Optical remote sensing data are an important source of geological information for regional mapping, tectonic structural interpretation of faults large-scale fractures and fracture zones (Suzen and Toprak, 1998; Wladis, 1999; Marghany and Hashim, 2010; Van Der Meer et al., 2012; Hashim et al., 2013).

Traditionally, lineament mapping is based on a visual or semi-automatic interpretation of geomorphological features, such as morphotectonic elements, drainage network offsets and

stream segment alignments, and/or spectral criterion, such as tonal changes, patterns and textures.

However, the accuracy of features detected ~~detection~~ from satellite images is affected by several factors including characteristics of the sensor, characteristics of the landform, lighting conditions, and cloud coverage (Smith and Wiseb, 2007). Illumination conditions can be affected by topography: the proportion of light reflected toward the satellite varies with the relative positions of the sun, target, and viewer, the geometry of which varies with topography (Shepherd and Dymond, 2003; Marghany and Hashim, 2010; Rahnama and Gloaguen, 2014). For this reason, the use of a Digital Elevation Model (DEM) or a Digital Terrain Model DTM, alone (Simpson and Anders, 1992; Byrd et al., 1994; Collet et al., 2000; Seleem, 2013) or in combination with remotely sensed images on regional scale (Florinsky, 1998; Chorowicz et al., 1999; Jacques et al., 2012), provides ~~is~~ a useful alternative technique for lineament extraction that avoids most of the limiting factors discussed above (Moore et al., 1991; Jordan et al., 2005; Masoud and Koike, 2011). Faults and linear features can be detected and quantified using terrain parameters extracted from a DTM, such as elevation, slope and convexity (curvature). Morphology characterization is based on slope profiles, curvature values, spatial distribution of homogeneous areas, and cumulative frequency analysis of terrain distribution (Evans, 1980; Jordan et al., 2003; Jordan et al., 2005). For example, curvature maps and slope maps can be used to recognize change in slope gradient, and consequently to identify fault lineaments distribution (Ganas et al., 2005; Jordan et al., 2005). The literature presents several methods based on gridded data of DTMs and DEMs for calculating terrain parameters (Moore at el., 1991; Wise, 2000; Shary et al., 2002; Kienzle, 2004).

In this paper, we propose the application of a new semi-automatic approach based on DTMs for the extraction of potential lineaments. The approach tested here was originally developed (Umili et al., 2013) to automatically detect discontinuity traces in rock outcrops to evaluate

their degree of fracturing (Umili et al., 2013; Ferrero et al., 2014). In this paper, the method is expanded for feature extraction over a larger area. As a first test area, we selected the Monferrato domain (NW Italy), part of the Tertiary Piedmont Basin (TPB). Significant results have been obtained showing the effectiveness of CurvaTool software for preliminary assessment of potential geological lineaments (Bonetto et al., 2015). Here we further discuss the functionality and applicability of the CurvaTool method in another test area with different accessibility and geological conditions. We selected an area in the Bagni di Vinadio municipality (Cuneo, NW Italy), which is part of the Argentera Massif (Western Alps), as a test site to apply the CurvaTool method on a 10 m ground spatial resolution DTM (source Piedmont Region GeoNetwork). We selected this mountainous area for several reasons, including problematic accessibility, interest in the geothermal features of the area, and availability of data from the literature. Data obtained from the CurvaTool code (Umili et al., 2013) have been successively compared with literature information and visually extracted lineaments from ortho-photos (Source Arpa Piemonte – data acquisition October 2000).

2 – THE ARGENTERA MASSIF

The Argentera Massif (AM) is in the Western Alps and belongs to the External Crystalline Massifs. It crops out in the footwall of the Penninic Frontal Thrust (Figure 1), and is divided into two main complexes: the Tinée Complex (TC) and the Malinvern-Argentera Complex (MAC), which represent the western and eastern portions of the massif, respectively.

Figure 1 here

The AM is characterized by high grade metamorphic rocks (schist, paragneiss, amphibolites, diatexite and anatectic granitoid), locally intruded by post-metamorphic granitic bodies (Fry, 1989; Bogdanoff et al., 2000). The crystalline rocks are unconformably overlain by Triassic to Early Cretaceous carbonates, that are mostly detached above Late Triassic evaporites with the basement-cover contact mainly striking NW-SE (Guglielmetti et al., 2013). AM is characterized by Alpine stage ductile shear zones and strike-slip and reverse faults, resulting from brittle reactivations of networks of structures of pre-Alpine and early-Alpine age (Bogdanoff et al., 1991; Musumeci and Colombo, 2002; Corsini et al., 2004; Guglielmetti et al., 2013). Many faults belong to a NW-SE system that mainly consists of right-lateral, high angle strike-slip faults; a conjugate of left-lateral, NE-SW trending system is also present, locally turning to the ENE-WSW (Baietto et al., 2009). In particular, three main high angle shear zones cross the AM: the Valletta shear zone (VSZ), the Bersezio fault zone (BFZ) and the Fremamorta shear zone (FMS) (Figure 1). The FMS cuts the center-southernmost portion of the AM, connecting toward north to the BFZ, which consists of a dense set of faults striking NW–SE (Guglielmetti, 2012). The VSZ and the BFZ run parallel to each other in the northern sector of the AM. They are NW-SE oriented and define a 3-km-wide continuous belt made up of high angle strike-slip faults both NW–SE to NNW–SSE and NE–SW to ENE–WSW trending (Baietto et al., 2009; Guglielmetti et al., 2013). The VSZ corresponds to the contact between the TC and MAC, and is represented by an up to one-kilometer-thick mylonitic rock layer formed during a pre-Alpine deformation stage with a dextral strike-slip trend (Musumeci and Colombo, 2002; Guglielmetti et al., 2013). Triassic sedimentary cover uncomfortably overlies the basement rocks along the Sespoul, La Blance and Tortissa thrusts (Bogdanoff et al., 2000).

Seismic and GPS data show that the area is still tectonically active, with crustal shortening of 2-4 mm/year induced by N-S to NE-SW compression (Madeddu et al., 1996; Ribolini and Spagnolo, 2008), especially in the axial region of the massif (Perello et al., 2001). The continuing crustal mobility of the Argentera is also indicated by Permanent Scatterers (PS) data (Morelli at al., 2011).

The Bagni di Vinadio test area is in the northwestern part of the AM, corresponding with the transition between TC from the west and the MAC from the east (Figure 2). The BFZ and VSZ are the main structures in the area. Migmatitic gneisses, fine-grained aplitic granites and minor slices of sedimentary rocks mainly occur in the center and south portion of the test area, whereas the sedimentary cover and Permo-Triassic crystalline basement crop out in the northeaster sector of the tested area (Guglielmetti et al., 2013).

Figure 2 here

3 - METHODOLOGY

We first analyzed the test site (Figure 3) by visual detection of linear features, and then with the CurvaTool code (Umili et al., 2013). Results were compared and related to data from the literature. We performed visual lineament extraction on a set of ortho-photos, called "Flight Flood 2000", commissioned by Piedmont Region (http://webgis.arpa.piemonte.it/joomla_gpa_32/) after the flood of October 2000: aerial

images (ground spatial resolution of 2.5 m) were collected during autumn 2000 in the north sector of Piedmont and during spring 2001 in its south sector.

Figure 3 here

Visual identification of lineaments is mainly based on the experience of the operator. Two criteria were applied to identify lineaments: (i) geomorphological and (ii) tonality criterion. Geomorphological criterion is based on the identification of morpho-tectonic and drainage elements, such as rectilinear or segmented patterns of valleys, scarps and ridges, drainage pattern offsets, and stream-segment alignments. Tonality criterion is based on the visual interpretation of differences in color tones and light contrast. Tonality, in fact, varies as a function of differences in vegetation, lithology, soil water content, permeability and rock strength (O'Leary et al., 1976). Since the identification of lineaments can be affected by changes in the illumination azimuth and slope, the ortho-photos were enhanced by overlaying the DTM elevation contour map to show the exact location of valleys, ridges and slope breaks.

The CurvaTool code semi-automatic method for lineament identification is based on the assumption that a geological lineament can be geometrically identified as a convex or concave edge of a DTM, particularly where there is structural control of the geomorphological evolution of the analyzed area. A detailed description of the working principles and calculation methods of CurvaTool code can be found in Bonetto et al. (2015).

A DTM (ground resolution of 1 point every 20 m), containing the same area as the one covered by the previously described ortho-photos, was used as input for the CurvaTool code (Umili et al., 2013). Since the area is mountainous, with an elevation difference of 2,130 m, the DTM surface contains a large number of recognizable crests and valleys. Therefore, the area is suitable for semi-automatic linear feature extraction by the CurvaTool code. The code

is based on an estimate of principal curvature values (maximum and minimum) associated with each DTM point, thus implementing the method proposed by Chen and Schmitt (1992) and extended by Dong and Wang (2005). As briefly illustrated by the flow chart in Figure 4, the user is asked for two thresholds: the first one, called Tmax, represents the minimum acceptable value of maximum principal curvature (kmax) to select DTM points potentially belonging to significant convex edges (e.g. crests); the second, called Tmin, represents the maximum acceptable value of minimum principal curvature (kmin) to select DTM points potentially belonging to significant concave edges (e.g. valleys). After a process of points linking, each resulting polyline is segmented: each obtained segment is measured and its angle with respect to North direction is calculated.

Figure 4 here

The quality of the DTM is fundamental (Kraus, 1993; Kraus and Pfeifer, 1998): the smaller the mean distance between adjacent points, the better the correspondence between the discretized surface and the actual ground surface, and the lower the smoothing effect. The method works particularly well on models with a wide range of principal curvature values, that is on surfaces with a high degree of non-planarity.

Once linear feature extraction has been performed, post-processing operations are required in order to obtain significant results; therefore, the algorithm called "Filter" has been specifically created by the authors to perform operations on the linear features database (Figure 5). Post-processing can follow two different approaches, based on the degree of knowledge of the area and on the purposes of the study. The first approach is applicable in case no literature data are available for the studied area: in this case a frequency analysis is performed on liner features directions; by analyzing the obtained rosette of directions the user can make considerations useful for a preliminary tectonic assessment. In case the area is already geologically well-

known and literature data are available for the studied area, in terms of mean direction of lineaments sets, post-processing starts with a comparison with literature data: the user has to assign the minimum lineament length and the orientations of the expected clusters of lineaments (expressed by an angle with respect to the North and its standard deviation). The Filter code deletes linear features shorter than the fixed length and classifies the each remaining edge, attributing it to the correspondent input cluster. Non-classified features are recorded as "others" (Bonetto et al., 2015). Then, operations of mapping and statistical analysis of lineaments length can be performed on the obtained database.

then

Figure 5 here

4 – RESULTS AND DISCUSSION

identified

A large number of linear features were found in our test area: 1,848 from visual extraction and 8,465 by the CurvaTool software (Figure 6). The number of linear features extracted by CurvaTool is remarkable with respect to the number identified by visual extraction. The 3D geometrical approach implemented in the software allows CurvaTool to identify all concave or convex edges of the ground surface, while visual extraction is subjective and strictly depends on the experience and ability of the analyst and the observation scale. Moreover, some variations of surface edge are not visually detectable, but while they can be geometrically described in terms of curvature and therefore analysed by the code.

However

On the other hand, a few remarks must be made on the possibility that some of the extracted linear features could be false lineaments, that is natural or artificial linear elements that do not

represent geological lineaments. First of all, the resolution of the DTM plays an important role: in fact, every false lineament whose dimensions are smaller or similar to the ground resolution is not - or only partially- represented by the DTM; therefore it is not detectable as a linear feature by CurvaTool. Considering that a 5 m resolution DTM is already a very detailed model for our purposes, this means that it's likely that canals and river banks would not be observable on its surface. Moreover, the most common artificial linear elements, such as roads and railroads, are almost flat and therefore, even if detectable on the DTM surface, they belong to areas characterized by non-significant curvature values. However, the possibility that a few linear features representing false lineaments could be detected exists; therefore, a geologically based reasoning must be made in this sense. Generally, main faults are not isolated structures: the area in which a fault is located is usually characterized by a structural arrangement that reproduces the fault direction. Moreover, our purpose is not only to create a lineament map, but is to obtain information about the average direction of lineament sets, instead. Therefore, a single false lineament cannot invalidate the result of the cluster analysis performed on all the extracted linear features.

Getting back to results discussion, all the detected lineaments were statistically analyzed to compare them in terms of quantity, orientation and geographical distribution.

Figure 6 here

Filter was applied to both the semi-automatic and visual methods to perform a cluster analysis and correctly assign linear features into different sets (Bonetto et al., 2015). Four set orientations were assigned, according to geomorphological and structural literature data (Baietto et al., 2009; Guglielmetti et al., 2013) (Table 1).

Table 1 here

The acronym TELF is assigned to indicate the Total Extracted Linear Features. Using visual extraction (Table 2), NW-SE lineaments (L1) are less frequent (9.42% of TELF), and are mainly in the southern area; NE-SW lineaments (L2) are the most numerous (19.32% of TELF), and show a principal distribution in the center and south areas. N-S (L3) and E-W lineaments (L4) show a similar frequency (nearly 18% of TELF both for L3 and L4), and are mainly in the northern area. Some linear features do not correspond to the orientation indicated in Filter: they represent 36% of TELF.

Table 2 here

For the results of the CurvaTool processing (Table 3), the NW-SE set (L1) shows a high frequency (20% of TELF) and uniform distribution in the test area; the NE-SW set (L2) is less frequent (11.79% of TELF) and is chiefly distributed in the center and south-west of the test area. The N-S lineaments (L3) are predominant (20.58% of TELF) and show a homogeneous distribution in the whole area. The E-W set (L4) shows a slightly smaller frequency (20.20 % of TELF), and was mainly identified in the northern and south-eastern area. The linear features found with CurvaTool that are not included in the range assigned to Filter represent 27% of total features.

Table 3 here

In Figure 7 the different sets have been separated to better compare linear features extracted by visual analysis and CT processing. Despite the high number of linear features detected, the percentage of unassigned lineaments identified by CurvaTool (27.43%) is lower than that obtained from visual approach (31.54%). Comparing the percentage of linear features assigned to each set, the main difference between CurvaTool and visual extraction is in the L1 and L2 sets (Table 4).

Figure 7 here

Table 4 here

The sets used in Filter correspond to the orientations of the main geological lineaments in the Argentera Massif; in particular, L1 and L2 correspond to the two main observed conjugate systems that are associated with NW-SE striking thrusts and faults. The NE-SW system (L2) is minor and discontinuous. Set L1 is dominant: it reactivates pre-existing shear zones and pre-alpine foliations in the basement. Also, the basement–cover contact strikes NW-SE (Perello et al., 2001; Baietto et al., 2009). Comparing semi-automatic and visual processing, CurvaTool underestimates the importance of L1, whereas visual extraction overrates L2. This disparity is probably due to the drainage network in the test area, which is strictly related to geological lineaments orientation, thus conditioning the detection of linear features. In the test area, most of the main rivers and first order stream channels are NW-SE elongated, and show a flat floor. Since DTM points in open valleys correspond to very low and uniform values of curvature, it is likely that they were discarded from the analysis during the choice of curvature thresholds for CurvaTool. The CurvaTool technique is called semi-automatic because the user is asked for two thresholds: minimum and maximum principal curvature values that discriminate between significant and insignificant edges. Therefore, very flat areas are not considered significant for edge identification. However, where the orientation of low-order channels corresponds to a NW-SE strike, both CurvaTool and visual extraction identify linear features belonging to set L1.

As reported in Ribolini and Spagnolo (2008), in some portions of the test area, for example along the Stura River, several low-order channels run perpendicular to both the main river stem and geological lineaments as well. This type of drainage pattern, where present, could

be the cause of the high number of linear features assigned to L2, particularly by visual extraction where subjectivity and main morphological elements influence the process. Musso et al. (2009) notice that, in the AM, geomorphic evolution is particularly controlled by a NE-SW normal fault system consisting of relatively short segments. Therefore, the influence of morphological criterion on the visual interpretation, is likely the reason for the high percentage of L2 lineaments identified by visual extraction, despite the secondary relevance of this set to L1. Most of the linear features detected by CurvaTool belonging to L1 and L2 are short segments aligned along the NW-SE and NE-SW directions respectively. Perello et al. (2001) describes the NW-SE and NE-SW striking systems as discontinuous high angle faults. L3 and L4 have similar percentage values in both the analytical approaches. Field geological mapping and literature data (Malaroda et al., 1970; Crema et al., 1971; Perello et al., 2001; Baietto et al., 2009; Guglielmetti, 2012), indicate the presence of geological lineaments striking E-W (L4). They are usually short and discontinuous, and frequently connect or displace faults belonging to the main NW-SE system. With regard to the ENE-WSW lineaments, they are associated with the conjugate system of NW-SE strike-slip faults (L2). CurvaTool and visual extraction also detect N-S striking linear features; no important structures with this orientation are known at regional scale in the study area, but detailed field data from Perello et al. (2001) reported the presence of faults with N-S orientation in the Bagni di Vinadio area, associated with low-angle shear zones. Guglielmetti (2012) identified N-S striking morphological elements using photointerpretation, particularly in the SE part of the AM (Terme di Vinadio area).

We observed a non-homogeneous distribution of linear features and different lineament domains, particularly using CurvaTool processing (Figure 8). Spatial distribution and alignment of linear features detected by both CurvaTool and visual analysis indicate quite

clearly the presence of two main lineaments, in the center and SW part of the test area. When compared to geological mapping data (Malaroda et al., 1970; Crema et al., 1971; Baietto et al., 2009; Guglielmetti, 2012), they correspond respectively to the Bersezio and Valletta faults. The anomalous concentration of NW-SE and NE-SW oriented linear features in the middle of these lineaments is due to the presence of the shear zone called "Bersezio Fault Zone" (area A in Figure 8 a, b). A change in spatial distribution and frequency of linear features was observed NE of the Stura River. The NE sector (area C in Figure 8 a, b) shows a homogeneous distribution of linear features with preferred NW-SE and E-W orientations, whereas the sector between this domain and the Stura River (area B in Figure 8 a, b) is characterized by a predominance of NE-SW linear features. The boundary between the two sectors seems to correspond to the NW-SE trending basement-cover contact. The south-eastern areas of Bagni di Vinadio town (area D in Figure 8 a, b), bounded on the northwest by the Corborant River, shows a predominance of L4 and L1 features. Part of this sector is geologically still included in the Bersezio fault zone, a complex system of anastomosing faults made of lens-shape tectonic slices (Perello et al., 2001) formed by NW-SE (L1), NE-SW (L2) and E-W (L4) lineaments. The domain boundaries, particularly as highlighted by CurvaTool, are NW-SE and NE-SW striking, coherent with both main fault directions and iso-kinematic boundaries defined with the PS-InSAR technique by Morelli et al. (2011). Iso-kinematic boundaries are mainly aligned along both a NW-SE direction, parallel or subparallel to the NW-SE transpressive faults, and a NE-SW direction, subparallel to the main drainage network and normal fault system (Musso et al., 2009). In the visual approach, it is possible to observe the same domains, but the above described limits are not as well defined compared to CurvaTool, probably because of the limited number of linear features detected (Figure 8b).

Figure 8 here

5 - CONCLUSIONS

The CurvaTool code has been applied to DTMs over large areas to semi-automatically detect edges, which represent potential geological linear features. To verify the results obtained by the software, CurvaTool outputs were compared to visually extracted linear features and also to geological literature data.

This study shows very well that CurvaTool processing permits extraction and classification of a greater number of linear features compared to visual interpretation. The ability to detect features not perceptible by visual observation is a strong point of CurvaTool processing. Visual interpretation is unable to detect short segments and less evident surface edges as well as CurvaTool; moreover, visual extraction is subjective and influenced by the experience of the analyst. The overall positive aspects of this semi-automatic process include the rapidity of preliminary assessment, the ability to identify the most interesting areas to be investigated, and to analyze areas that are not directly accessible. DTM resolution has a direct influence on lineament definition and completeness. The number of points on the surveyed surface and, consequently, the amplitude of the triangles of the digital model, influence the quality of the approximation of the real surface. In addition, a decrease in resolution results in "smoothing" and consequent deterioration of the edges of the surface. This reduces the range of principal curvatures and, depending on the triangulation, disrupts or alters the continuity of the edges.

In the test area, CurvaTool data are consistent with visually detected linear features, and show a good correlation with structural data (Malaroda et al., 1970; Perello et al., 2001; Corsini et al., 2004; Baietto et al., 2009) and iso-kinematic maps (Morelli et al., 2011), demonstrating the value of the semi-automatic approach. The abundance of linear features identified by CurvaTool allows for better identification of homogeneous domains (in terms of frequency and distribution of linear features). CurvaTool processing identifies the main faults and shear zones reported in the literature. The alignment of long, single segments and their high density in NW-SE elongated areas, corresponds with the location of the Bersezio and Valletta faults, their deformation zones and the basement-cover contact.

The semi-automatic method has the potential to detect main geomorphic and structural features at a regional scale, particularly in areas where tectonics has a strong control on geomorphic evolution. With regard to the NW sector of the AM, where Bagni di Vinadio is located, the lower relief results in a generally higher sensitivity of the drainage network to faults and fracture systems, which determines preferential orientation of the lineaments (Ribolini and Spagnolo, 2008).

Preliminary results of this research show that the application of the CurvaTool code to large areas can be a potential tool in preliminary geological and structural studies, particularly in areas that are not directly accessible or when scarce existing data are available. CurvaTool can give useful and rapid information about the orientation and spatial distribution of potential geological and geomorphological lineaments, and the possible presence of domains with homogeneous features and lineament distributions. Based on this approach, further specific field studies can be planned to verify these results.

In alpine environments, CurvaTool shows a high potential due to less quaternary cover obscuring tectonic elements, and it is easier to validate results because of the abundance of outcrops and field data. Further research in the test area will consist of statistical analysis of

the frequency distribution and length of the lineaments belonging to each set, and the influence of rock type on the linear feature detection. Subsequent investigations and statistical processing of the data are needed to validate and improve the software. Additionally, testing new areas with different tectonic and geomorphologic environments is also a future priority.

REFERENCES

Baietto, A.; Perello, P.; Cadoppi, P.; and Martinotti, G., 2009, Alpine tectonic evolution and thermal water circulations of the Argentera Massif (South-western Alps): *Swiss Journal Geosciences*, Vol. 102, pp. 223–245.

Bogdanoff, S.; Michard, A.; Mansour, M.; and Poupeau, G., 2000, Apatite fission tracks analysis in the Argentera massif: evidence of contrasting denudation rates in the external crystalline massifs of the Western Alps: *Terra Nova*, Vol. 12, pp. 117–125.

Bogdanoff, S.; Menot, R.; and Viviner, G., 1991, Les massifs cristallins externes des Alpes Occidentales francaises, un fragment de la zone interne varisque: *Science Geologique Bullettin*, Vol. 44, pp. 237–285.

Bonetto, S.; Facello, A.; Ferrero, A. M.; and Umili, G., 2015, A tool for semi-automatic linear feature detection based on DTM: *Computers & Geosciences*, Vol. 75, pp. 1–12.

Byrd, J. O. D.; Smith, R. B.; and Geissman, J. W., 1994, The Teton fault, Wyoming: neotectonics, and mechanisms of deformation: *Journal Geophysical Research*, Vol 99 (B10), pp. 20095–20122.

Chen, X. and Schmitt, F., 1992, Intrinsic surface properties from surface triangulation: Springer Berlin Heidelberg (Editor) *European Conference on Computer Vision*, pp. 739-743.

Chorowicz, J.; Dhont, D.; and Gundogdu, N., 1999, Neotectonics in the eastern North Anatolian fault region (Turkey) advocates crustal extension: mapping from SAR ERS imagery and Digital Elevation Model: *Journal Structural Geology*, Vol. 21, pp. 511–532.

Clark, C. D.; and Wilson, C., 1994, Spatial analysis of lineaments: *Computers & Geosciences*, Vol. 20 (7-8), pp. 1237–1258.

Collet, B.; Taud, H.; Parrot, J. F.; Bonavia, F.; and Chorowicz, J., 2000, A new kinematic approach for the Danakil block using a Digital Elevation Model representation: *Tectonophysics*, Vol. 316, pp. 343–357.

Corsini, M.; Ruffet, G.; and Caby, R., 2004, Alpine and late-hercynian geochronological constraints in the Argentera Massif (Western Alps): *Eclogae Geologicae Helvetiae*, Vol. 97, pp. 3–15.

Crema G.; Dal Piaz G.; Merlo C.; and Zanella E., 1971, Carta geologica d'Italia alla scala 1:100.000, Fogli Argentera, Dronero, Demonte, n. 78, 79 e 90 e Note illustrative: *Istituto Poligrafico e Zecca dello Stato - Archivi di Stato*, Roma [in Italian].

Davis, G. H. and Reynolds, S. J., 1996, *Structural geology of rocks and regions*: John Wiley & Sons, New York, 2nd Ed.

Dong, C.; and Wang, G., 2005, Curvatures estimation on triangular mesh: *Journal Zhejiang University Science*, Vol.6A (Suppl I), pp. 128-136.

Evans, I. S., 1980, An integrated system of terrain analysis and slope mapping: *Zeitschrift Geomorphologie*, Vol. 36, pp. 274-295.

Ferrero A. M., Migliazza M. R. and Umili G., 2014, Rock mass characterization by means of advanced survey methods. Keynote lecture. Rock Engineering and Rock Mechanics: Structures in and on Rock Masses: *Proceedings of EUROCK 2014, ISRM European Regional Symposium*, Vigo, Spain, 27-29 May 2014, pp. 17-27, ISBN 978-1-138-00149-7.

Florinsky, I. V., 1998, Combined analysis of digital terrain models and remotely sensed data in landscape investigations: *Progress Physical Geography,* Vol. 22, pp. 33–60.

Fry, N., 1989, Southwestward thrusting and tectonics of the western Alps. In: Coward, M. P., Dietrich, D., Park, R. G. (Editors.), *Alpine Tectonics: Geological Society of London, Special Publication.* Vol. 45, pp. 83–109.

Ganas, A.; Pavlides, S.; and Karastathis, V., 2005, DEM-based morphometry of range-front escarpments in Attica, central Greece, and its relation to fault slip rates: *Geomorphology*, Vol. 65, No. 3, pp. 301-319.

Guglielmetti L.; Comina C.; Abdelfettaha Y.; Schill E.; and Mandrone G., 2013, Integration of 3D geological modeling and gravity surveys for geothermal prospection in an Alpine region: *Tectonophysics*, Vol. 608, pp. 1025–1036.

Guglielmetti, L., 2012. *Multidisciplinary Approach of Geothermal Exploration in the Argentera Massif (Southwestern Alps):* PhD Thesis, Department of Earth Sciences, Torino University, Italy, 193 p.

Hashim, M.; Ahmad, S.; Johari, M. A. M.; and Pour, A. B., 2013, Automatic lineament extraction in a heavily vegetated region using Landsat Enhanced Thematic Mapper (ETM+) imagery: *Advances Space Research*, Vol. 51, No. 5, pp. 874–890.

Jacques, P. D.; Machado, R.; and Nummer, A. R., 2012, A comparison for a multiscale study of structural lineaments in southern Brazil: LANDSAT-7 ETM+ and shaded relief images from SRTM3-DEM: *Anais Academia Brasileira Ciências*, Vol. 84, No. 4, pp. 931-942.

Jordan G.; Meijninger B. M. L.; van Hinsbergen D. J. J.; Meulenkamp J. E.; and van Dijk P. M., 2005, Extraction of morphotectonic features from DEMs: development and applications for study areas in Hungary and NW Greece: *International Journal Applied Earth Observation Geoinformation*, Vol. 7, pp. 163–182.

Jordan, G.; Csillag, G.; Szucs, A.; and Qvarfort, U., 2003, Application of digital terrain modelling and GIS methods for the morphotectonic investigation of the Kali Basin, Hungary: *Zeitschrift Geomorphologie*, Vol. 47, pp. 145 - 169.

Kienzle, S., 2004, The effect of DEM raster resolution on first order, second order and compound terrain derivatives: *Transactions GIS*, Vol. 8, No. 1, pp. 83-111.

Kraus, K., 1993, *Photogrammetry, vol 1*, 4th ed.: Dummler, F. (Editor), Bonn. ISBN:3-427-78684-6.

Kraus, K.; and Pfeifer, N., 1998, Determination of terrain models in wooded areas with airborne laser scanner data: *ISPRS Journal Photogrammetry & Remote Sensing*, Vol. 53, No. 4, pp. 193–203.

Lee, M.; Morris, W.; Harris, J.; and Leblanc, G., 2012, An automatic network-extraction algorithm applied to magnetic survey data for the identification and extraction of geologic lineaments: *Leading Edge*, Vol. 31, No. 1, pp. 26–31.

Madeddu, B.; Bertoux, N.; and Stephan, J. F., 1996, Champ de contrainte post-pliocene et deformation recentes dans les Alpes sud-occidentales: *Bulletin Societe Geologique France*, Vol. 8, pp. 797–810.

Malaroda, R.; Carraro, F.; Dal Piaz, G. B.; Franceschetti, B.; Sturani, C.; and Zanella, E., 1970, Carta Geologica del Massiccio dell'Argentera alla scala 1:50.000 e Note Illustrative: *Memorie Società Geologica Italiana*, Vol. 9, pp. 557–663 [in Italian].

Marghany, M.; and Hashim, M. 2010, Lineament mapping using multispectral remote sensing satellite data research: *Journal Applied Sciences*, Vol. 5, No. 2, pp. 126-130.

Masoud, A.; and Koike, K., 2011, Morphotectonics inferred from the analysis of topographic lineaments autodetected from DMEs: application and validation for the Sinai Peninsula, Egypt: *Tectonophysics*, Vol. 510, pp. 291–308.

Moore, I. D.; Grayson, R. B.; and Ladson, A. R., 1991, Digital terrain modelling: a review of hydrological, geomorphological, and biological applications: *Hydrological processes*, Vol. 5, No. 1, pp. 3-30.

Morelli, M.; Piana, F.; Mallen, L.; Nicolò, G.; and Fioraso, G., 2011, Iso-kinematic maps from statistical analysis of PS-InSAR data of Piemonte, NW Italy: comparison with geological kinematic trends: *Remote Sensing Environment*, Vol. 115, No. 5, pp. 1188–1201.

Musso, A.; Piana, F.; Bertok, C.; d'Atri, A.; Martire, L.; Perotti, E.; and Varrone, D., 2009, Post-eocene transpression in Western Ligurian Alps: Geometry and kinematics of Limone-Viozene Deformation Zone (France-Italy border): *Epitome*, Vol. 3, pp. 181.

Musumeci, G.; and Colombo, F., 2002, Late Visean mylonitic granitoids in the Argentera Massif (western Alps, Italy): age and kinematic constraints on the Ferriere–Mollieres shear zone: *Comptes Rendus Geoscience*, Vol. 334, pp. 213–220.

O'Leary, D. W.; Friedman, J. D.; and Pohn, H. A., 1976, Lineament, linear, lineation: some proposed new standards for old terms: *Geological Society America* Bulletin, Vol. 87, No. 10, pp. 1463–1469.

Perello, P.; Marini, L.; Martinotti, G.; and Hunziker, C., 2001, The thermal circuits of the Argentera Massif (western Alps, Italy): an example of low enthalpy geothermal resources controlled by Neogene alpine tectonics: *Eclogae Geologicae Helvetiae*, Vol. 94, pp. 75–94.

Rahnama, M.; and Gloaguen, R., 2014, TecLines: a MATLAB-based toolbox for tectonic lineament analysis from satellite images and DEMs, part 1: Line segment detection and extraction: *Remote Sensing*, Vol. 6, No. 7, pp. 5938–5958.

Rangzan, K.; Charchi, A.; Abshirini, E.; and Dinger, J., 2008, Remote sensing and GIS approach for water-well site selection, southwest Iran: *Environmental & Engineering* Geoscience, Vol. 14, pp. 315–326.

Ribolini, A.; and Spagnolo, M., 2008, Drainage network geometry versus tectonics in the Argentera Massif (French–Italian Alps): *Geomorphology*, Vol. 93, pp. 253–266.

Shary, P. A.; Sharaya, L. S.; and Mitusov, A. V., 2002, Fundamental quantitative methods of land surface analysis: *Geoderma*, Vol. 107, No. 1, pp. 1-32.

Seleem T. A., 2013, Analysis and tectonic implication of DEM-derived structural lineaments, Sinai Peninsula, Egypt: *International Journal Geosciences*, Vol. 4, pp. 183-201.

Shepherd, J. D.; and Dymond, J. R., 2003, Correcting satellite imagery for the variance of reflectance and illumination with topography: *International Journal Remote Sensing*, Vol. 24, No. 17, pp. 3503–3514.

Simpson, D. W.; and Anders, M. H., 1992, Tectonics and topography of the Western United States - an application of digital mapping: *GSA Today*, Vol. 2, No. 6, pp. 117–121.

Smith, M. J.; and Wiseb, S. M., 2007, Problems of bias in mapping linear landforms from satellite imagery: *International Journal Applied Earth Observation Geoinformation*, Vol. 9, pp. 65–78.

Suzen, M. L.; and Toprak, V., 1998, Filtering of satellite images in geological lineament analyses: an application to a fault zone in Central Turkey: *International Journal of Remote Sensing*, Vol. 19, No. 6, pp. 1101–1114.

Umili, G.; Ferrero, A. M.; and Einstein, H. H., 2013, A new method for automatic discontinuity traces sampling on rock mass 3D model: *Computers & Geosciences*, Vol. 51, pp. 182–192.

Van der Meer, F. D.; Van der Werff, H. M. A.; Van Ruitenbeek, F. J. A.; Hecker, C. A.; Bakker, W. H.; Noomen, M. F.; Van der Meijde, M.; Carranza, E. J. M.; Boudewijn de Smeth, J.; and Woldai, T., 2012, Multi- and hyperspectral geologic remote sensing: A review: *International Journal Applied Earth Observation Geoinformation*, Vol. 14, No. 1, pp. 112-128.

Wise, S., 2000, Assessing the quality for hydrological applications of digital elevation models derived from contours: *Hydrological Processes*, Vol. 14, No. 11-12, pp. 1909-1929.

Wladis, D., 1999, Automatic lineament detection using digital elevation models with second derivative filters: *Photogrammetric Engineering & Remote Sensing*, Vol. 65, No. 4, pp. 453–458.

List of Tables:

Table 1 – Orientation of lineament sets used as input for Filter.

Table 2 –Statistics for visually extracted lineaments.

Table 3 – Statistics for lineaments obtained from CurvaTool processing.

Table 4 –Comparison between classified lineaments obtained from CurvaTool processing and visual interpretation.

List of Figures:

Figure 1 - Tectonic sketch map of the Argentera Massif and adjoining regions. BFZ: Bersezio fault zone, BF: Bersezio fault, VSZ: Valletta shear zone, FMS: Fremamorta shear zone. (source: Baietto et al., 2009). The box highlights the investigated area.

Figure 2 - Geological map of Bagni di Vinadio area (source: Guglielmetti et al., 2013).

Too small to be legible - enlarge to full page size.

Figure 3 – Test area: Bagni di Vinadio, Argentera Massif. Base map: orto-photo Flight Flood 2000 (source: Arpa Piemonte)

Figure 4 – Flow chart representing CurvaTool process

Figure 5 – Flow chart representing Filter process – figure blanked out.

Figure 6- Maps of lineaments of Bagni di Vinadio obtained from visual extraction (a) and by CurvaTool processing (b). figure 6a partially blanked out

Figure 7- Map of linear features of Bagni di Vinadio extracted and processed with Filter. Four sets are highlighted: (a) L1 (NW-SE), (b) L2 (NE-SW), (c) L3 (N-S) and (d) L4 (E-W). – obscured

Figure 8 - Main geological lineaments obtained by (a) visual extraction and (b) CurvaTool, and then processed with Filter. Areas characterized by an homogeneous/specific linear feature distribution are indicated as domains A, B, C, D.

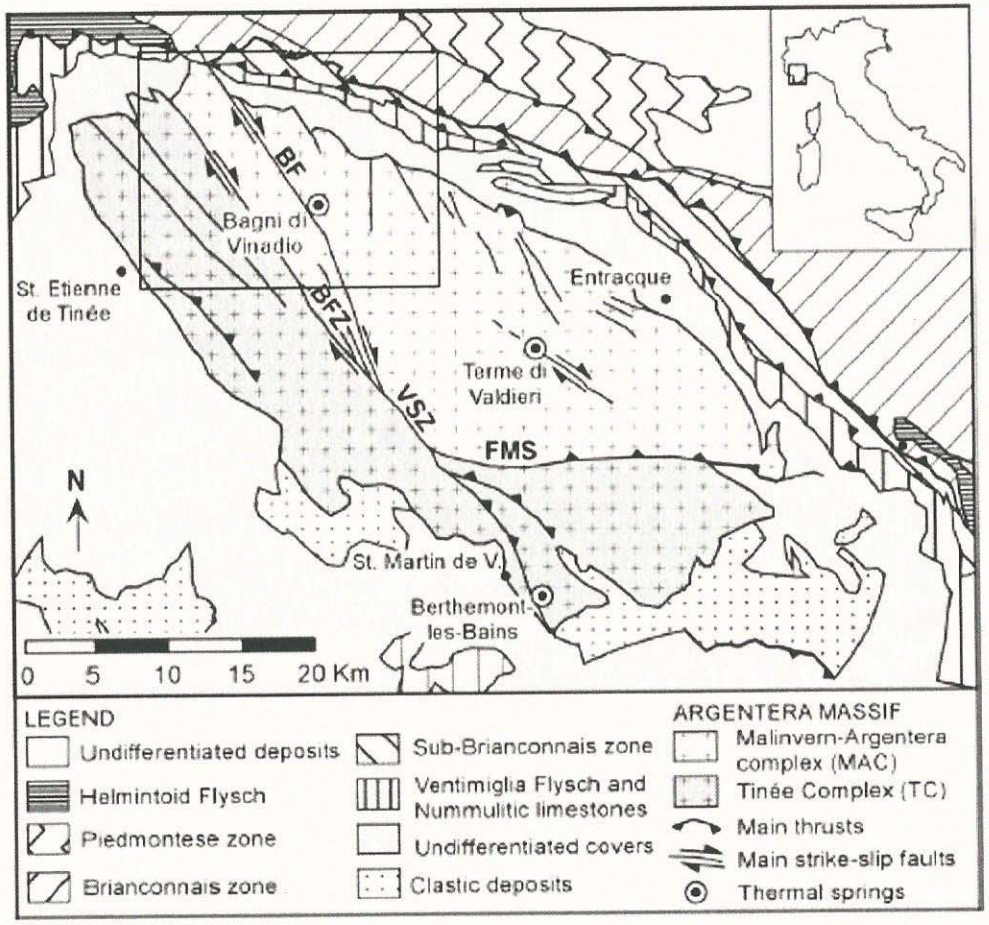
BF
Bagni di Vinadio
St. Etienne de Tinée
BFZ
VSZ
Entracque
Terme di Valdieri
FMS
N
St. Martin de V.
Berthemont-les-Bains
0 5 10 15 20 Km
LEGEND
Undifferentiated deposits
Helmintoid Flysch
Piedmontese zone
Brianconnais zone
Sub-Brianconnais zone
Ventimiglia Flysch and Nummulitic limestones
Undifferentiated covers
Clastic deposits
ARGENTERA MASSIF
Malinvern-Argentera complex (MAC)
Tinée Complex (TC)
Main thrusts
Main strike-slip faults
Thermal springs

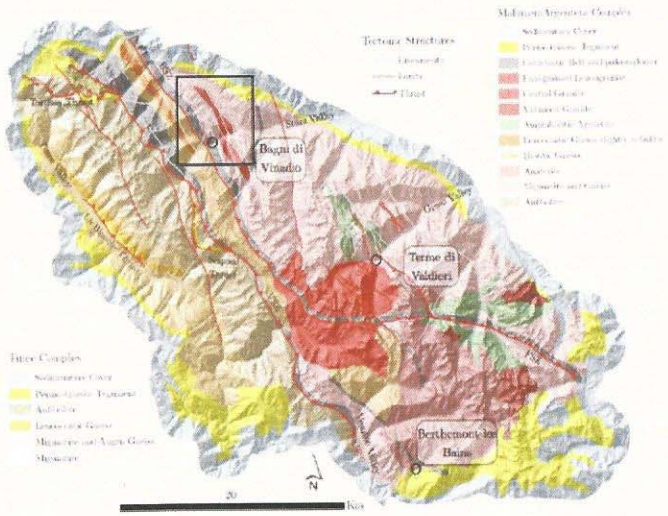

too small - make full page size.

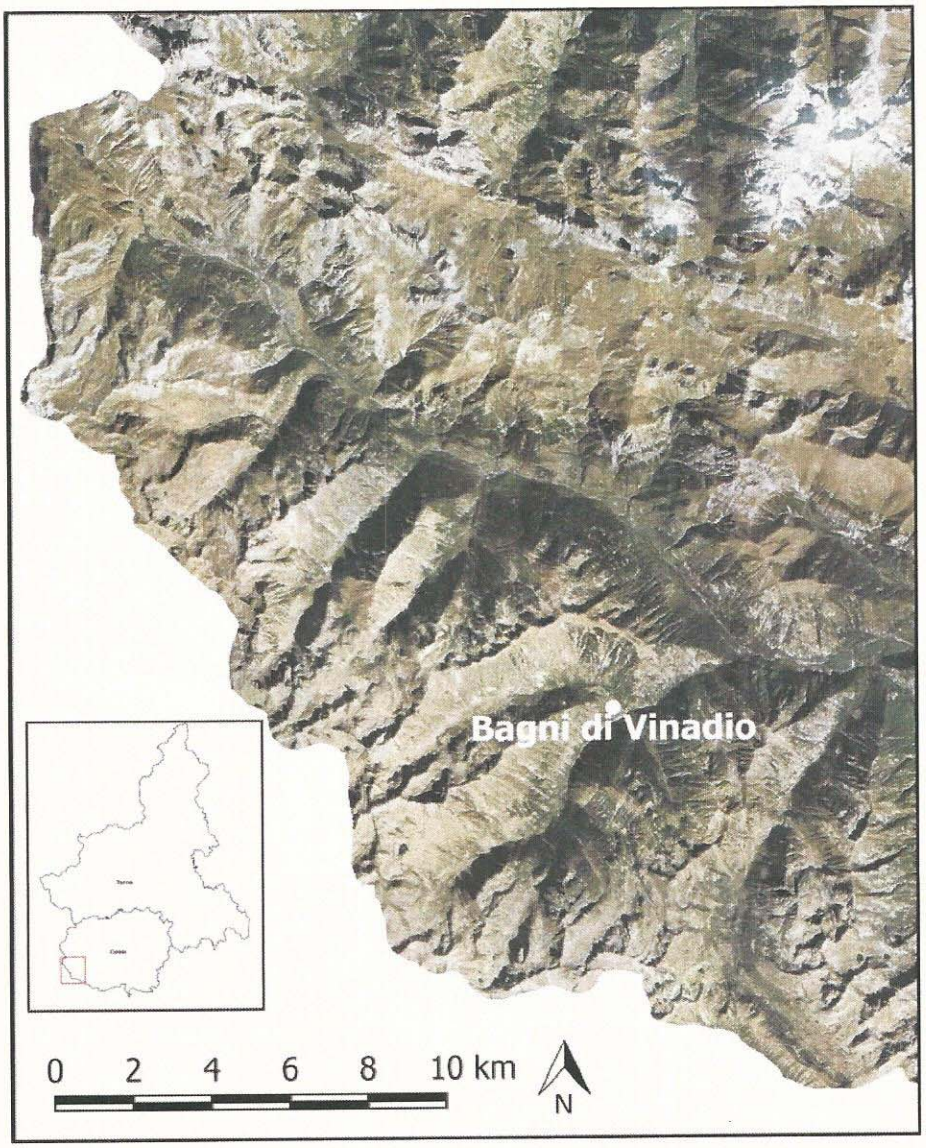
Bagni di Vinadio
0 2 4 6 8 10 km
N

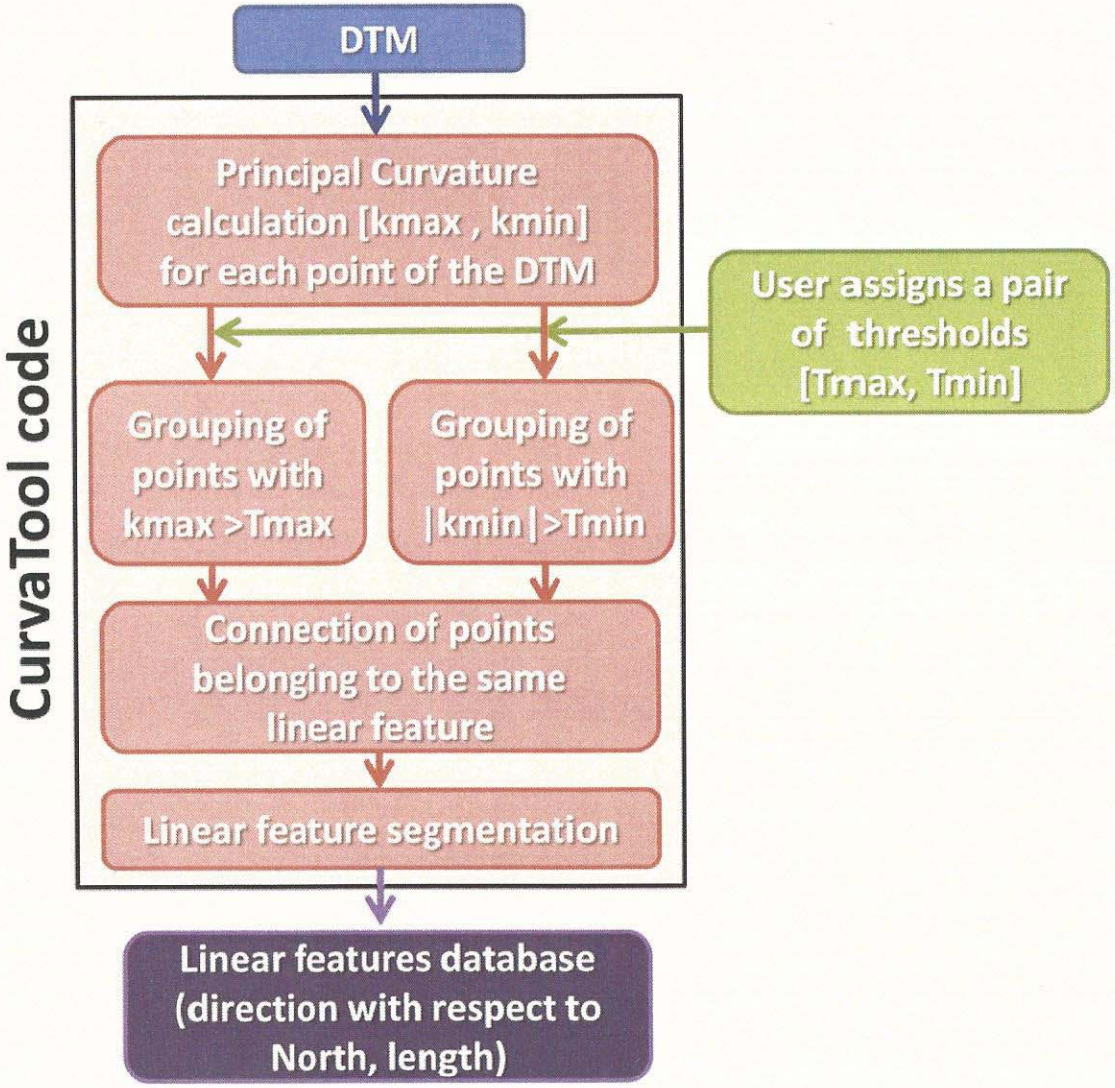
DTM
CurvaTool code
Principal Curvature calculation [kmax , kmin] for each point of the DTM
User assigns a pair of thresholds [Tmax, Tmin]
Grouping of points with kmax >Tmax
Grouping of points with |kmin|>Tmin
Connection of points belonging to the same linear feature
Linear feature segmentation
Linear features database (direction with respect to North, length)

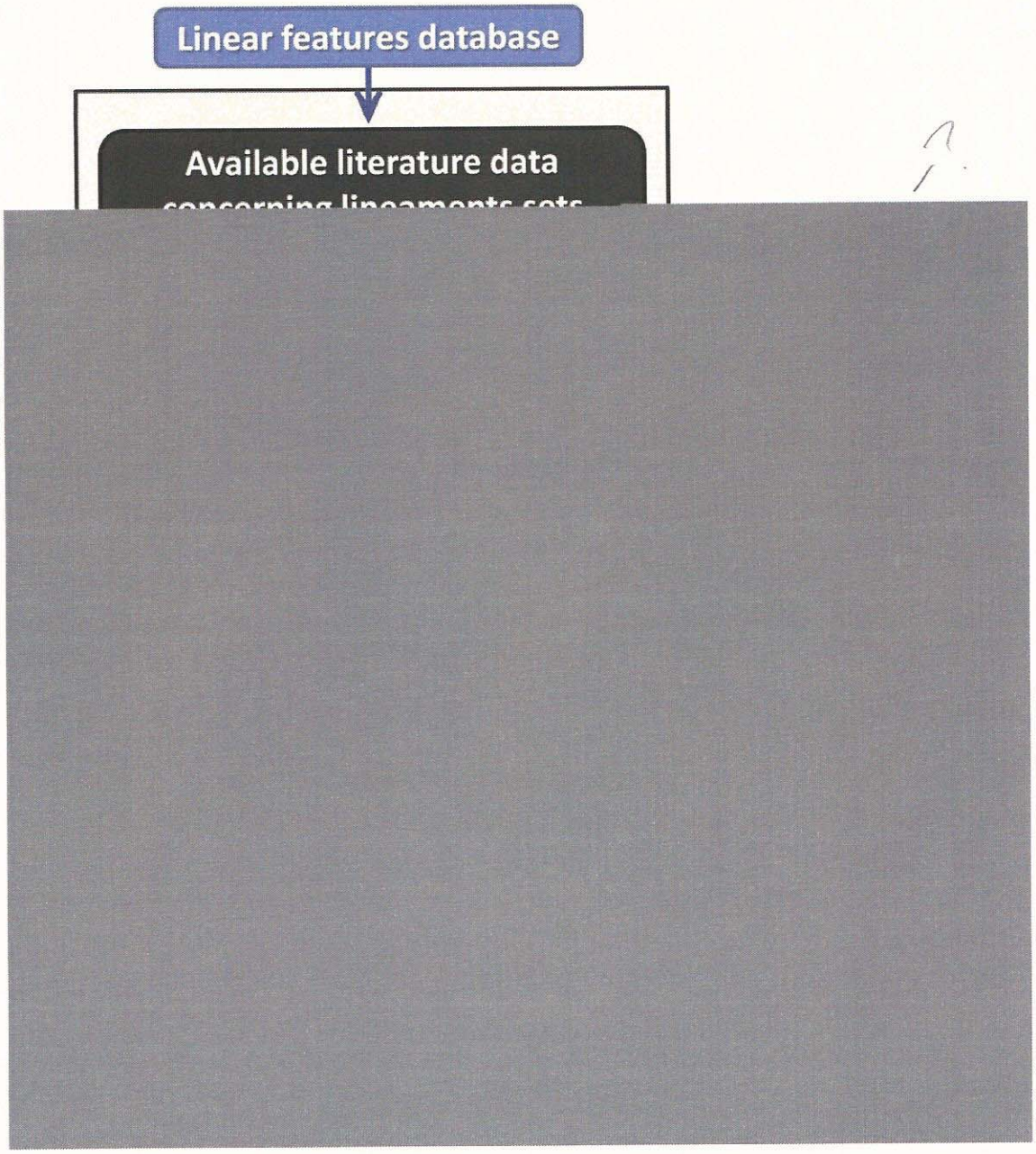
Linear features database
Available literature data

?

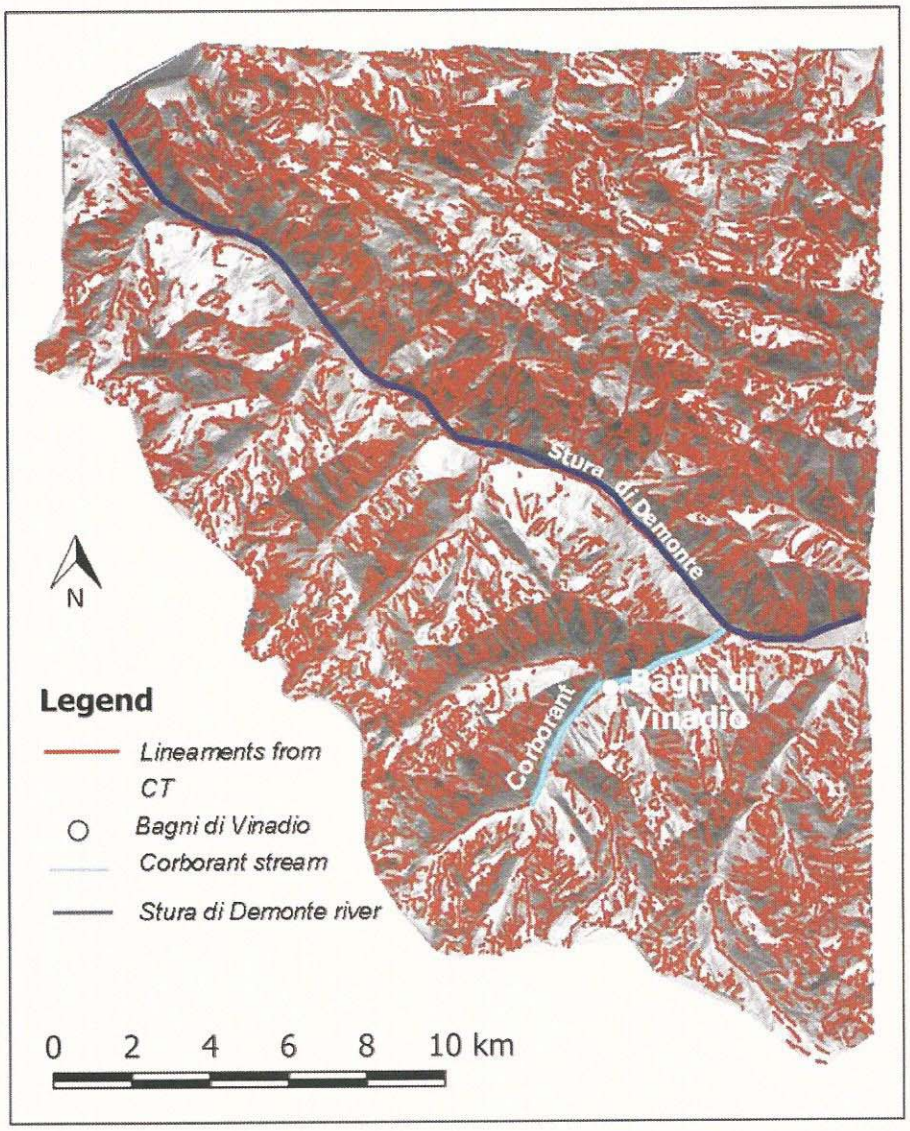
Stura di Demonte
Corborant
Bagni di Vinadio
N
Legend
Lineaments from CT
Bagni di Vinadio
Corborant stream
Stura di Demonte river
0 2 4 6 8 10 km

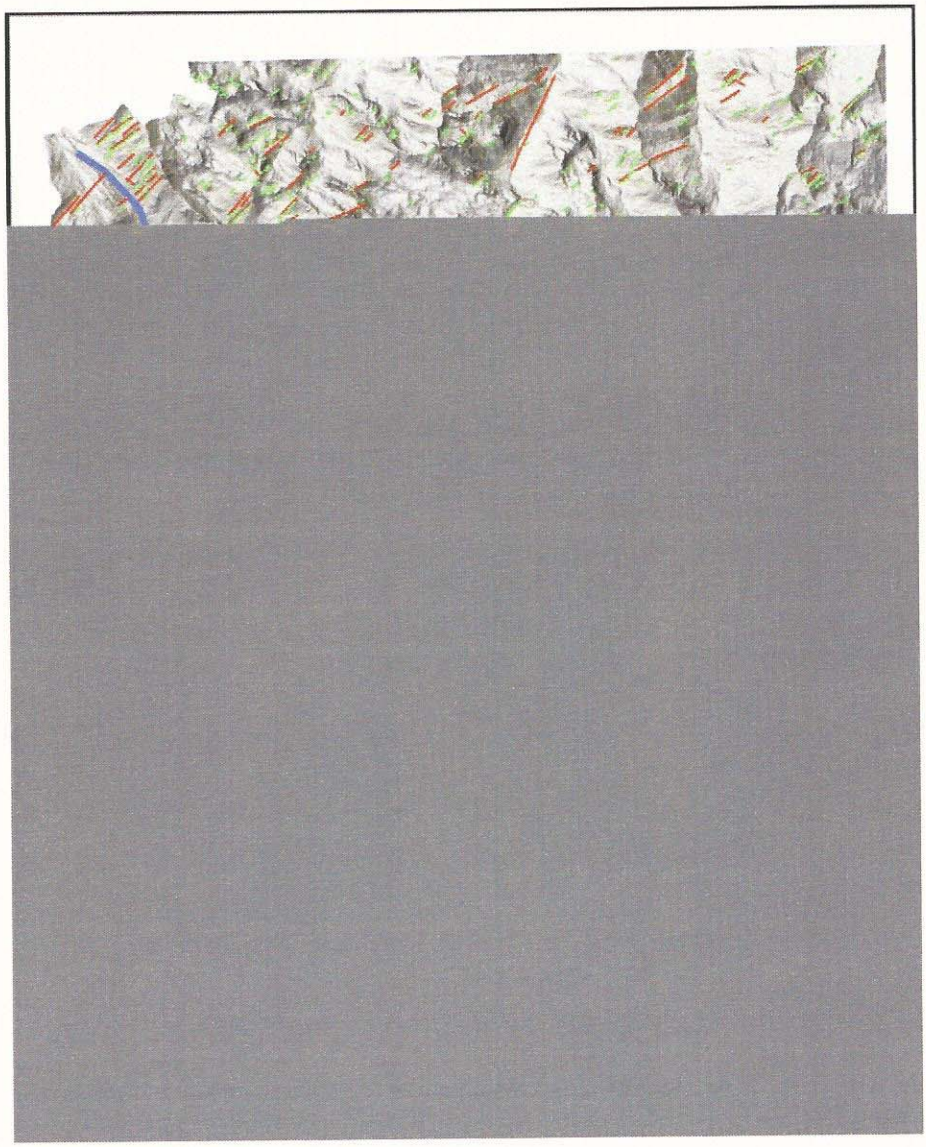

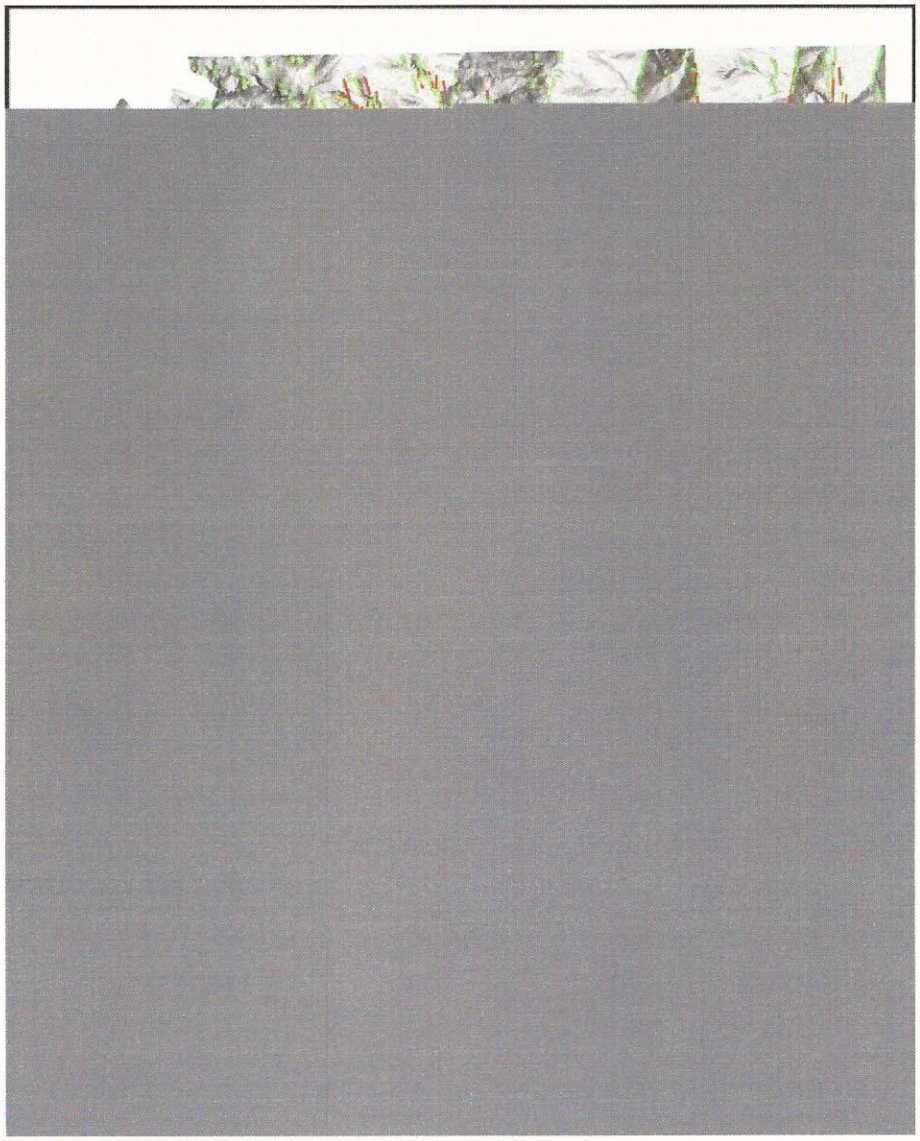

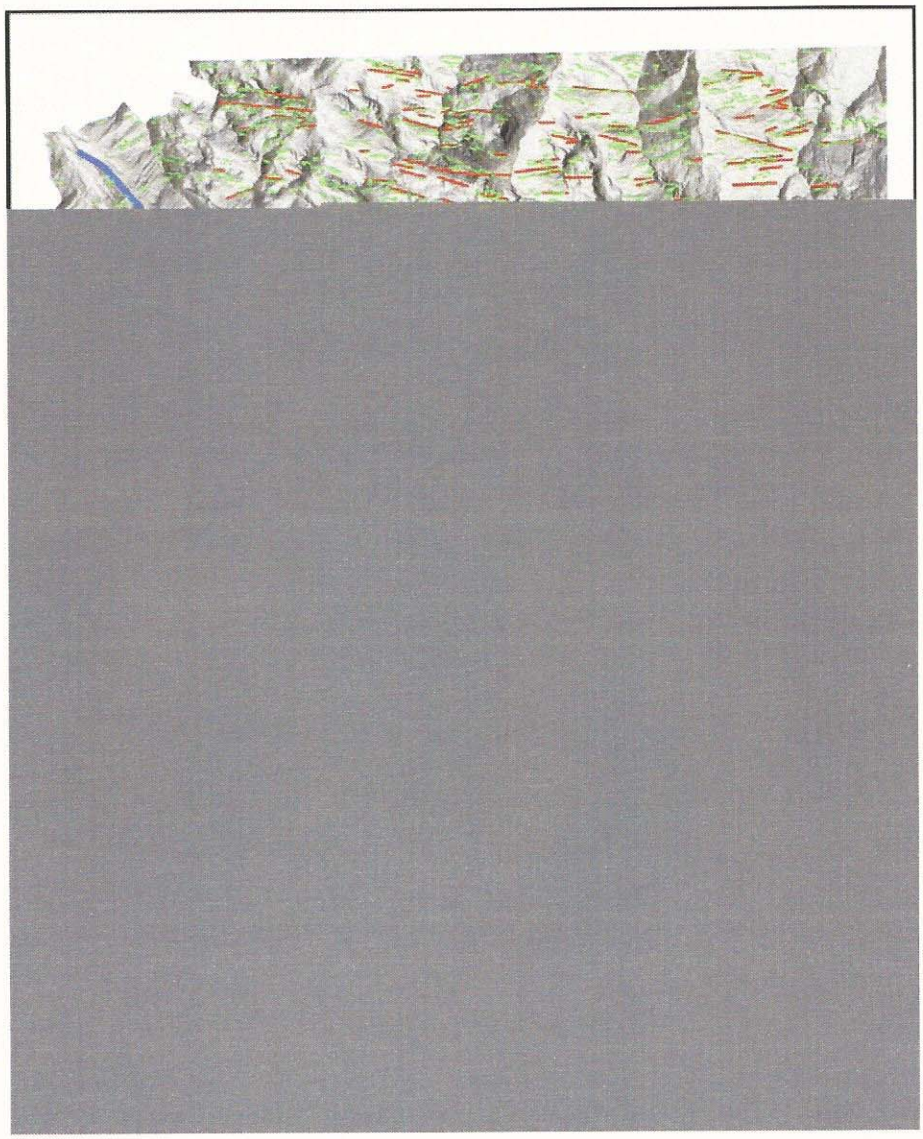

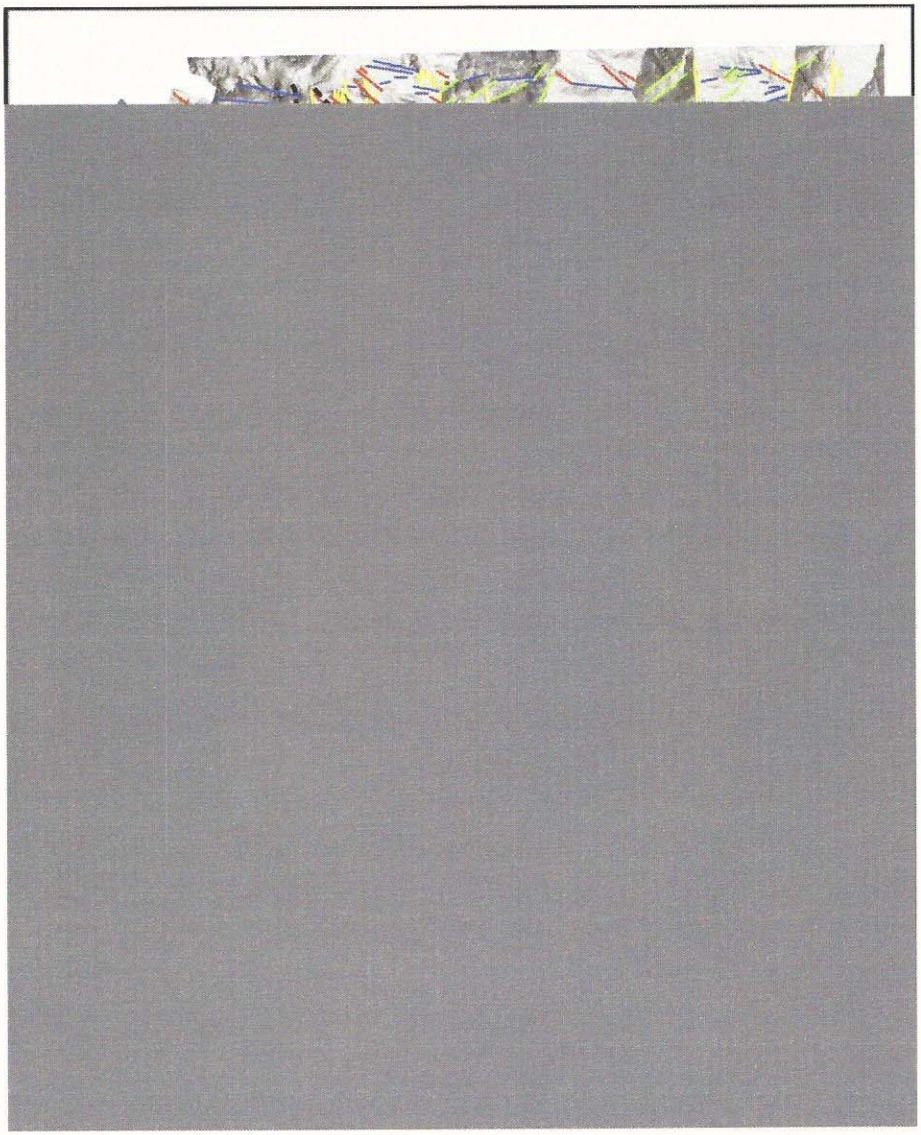

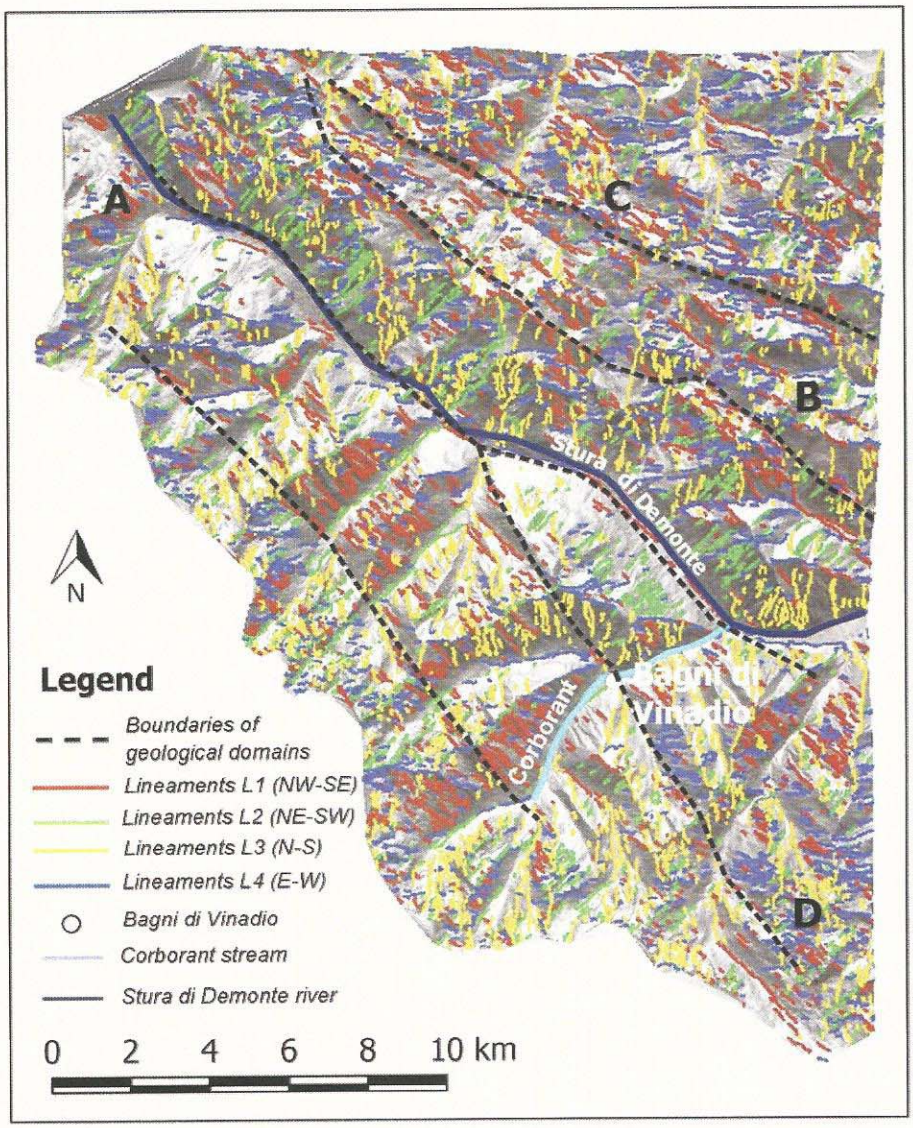
A
B
C
D
Stura di Demonte
Corborant
Bagni di Vinadio
N
Legend
Boundaries of geological domains
Lineaments L1 (NW-SE)
Lineaments L2 (NE-SW)
Lineaments L3 (N-S)
Lineaments L4 (E-W)
Bagni di Vinadio
Corborant stream
Stura di Demonte river
0 2 4 6 8 10 km

Table 1 – Orientation of lineament sets used as input for Filter.

Set	Azimuthal Direction [deg]	Standard Deviation [deg]
L1	N125	15
L2	N50	10
L3	N0	20
L4	N90	19.99

Table 2 –Statistics for visually extracted lineaments.

		Azimuthal Direction [deg]			
Set	**n° Lineaments**	**Minimum**	**Maximum**	**Mean**	**Standard Deviation**
L1	174	110.05	139.90	124.85	8.39
L2	357	40.24	59.86	49.38	5.36
L3	331	0.00	19.98	0.23	11.12
L4	329	70.02	109.98	87.56	10.62

Table 3 – Statistics for lineaments obtained from CurvaTool processing.

\		Azimuthal Direction [deg]			
Set	**n° Lineaments**	**Minimum**	**Maximum**	**Mean**	**Standard Deviation**
L1	1693	110.10	139.99	126.66	8.36
L2	998	40.10	59.94	49.77	5.65
L3	1742	-19.98	19.98	-0.89	11.76
L4	1710	70.02	109.98	90.43	11.59

Table 4 – Comparison between classified lineaments obtained from CurvaTool processing and visual interpretation.

Set	Percentage of total linear features (8465) extracted by CurvaTool	Percentage of total linear features (1883) visually extracted
L1	20.00%	11.78%
L2	11.79%	21.93%
L3	20.58%	17.57%
L4	20.20%	17.15%
Not Assigned	27.43%	31.54%